

## Relaxometric, Thermodynamic and Kinetic Studies of Lanthanide(III) Complexes of DO3A-Based Propylphosphonates

Ilgar Mamedov,<sup>\*[a]</sup> Petr Táborský,<sup>[b]</sup> Přemysl Lubal,<sup>\*[b]</sup> Sophie Laurent,<sup>[c]</sup> Luce Vander Elst,<sup>[c]</sup> Hermann A. Mayer,<sup>[d]</sup> Nikos K. Logothetis,<sup>[a,e]</sup> and Goran Angelovski<sup>\*[a]</sup>

**Keywords:** Lanthanides / Phosphonates / Kinetics / Thermodynamics / Contrast agents

Two DO3A-based ligands appended with the propylphosphonate side arm and their  $\text{Ln}^{3+}$  complexes were investigated. Proton relaxometric in vitro studies at 20 MHz and 60 MHz and 37 °C of the  $\text{Gd}^{3+}$  complex containing free acid exhibited relative changes of up to 56 % in  $r_1$  relaxivity when the pH of the medium was changed from 4 to 7. This change is explained by the decrease in the number of coordinated water molecules from two to one. Temperature-dependent relaxivity and NMRD profiles of  $\text{Gd}^{3+}$  complexes showed a

fast water exchange and a slightly increased rotational correlation time, which is characteristic of phosphonate-containing compounds. Thermodynamic and kinetic studies of the  $\text{Gd}^{3+}$  and  $\text{Eu}^{3+}$  complexes were performed by means of potentiometry and luminescence spectroscopy. The results indicate that the thermodynamic stability and kinetic inertness of these complexes are sufficient for their in vivo application. (© Wiley-VCH Verlag GmbH & Co. KGaA, 69451 Weinheim, Germany, 2009)

### Introduction

Magnetic resonance contrast agents (CA) based on  $\text{Gd}^{3+}$  chelates increase the relaxation rate of the surrounding water protons thus making them appear as a bright spot of amplified intensity in  $T_1$ -weighted images. The resulting improved sensitivity and markedly enhanced contrast of images obtained has led to the widespread use of magnetic resonance imaging (MRI) as an imaging technique in clinical and experimental settings.<sup>[1,2]</sup> However, the use of  $\text{Gd}^{3+}$  as a contrast agent is limited because of its high intrinsic toxicity. The size of  $\text{Gd}^{3+}$  is similar to that of  $\text{Ca}^{2+}$ , thus enabling it to interfere with the role of  $\text{Ca}^{2+}$  in the organism and disrupt  $\text{Ca}^{2+}$ -related signalling.<sup>[3]</sup> To this end, thermodynamically stable and kinetically inert complexes with  $\text{Gd}^{3+}$  chelators are required to prevent any dissociation of

the metal ions in the tissue,<sup>[4,5]</sup> resulting in numerous reports dedicated to studies of the thermodynamic stability<sup>[6,7]</sup> and the kinetic inertness of the potential CA.<sup>[8–10]</sup>

Besides the large amount of attention given to the requirements related to the stability of complexes, the design of novel CA for possible application in MRI has also concentrated on the development of high relaxivity agents.<sup>[11,12]</sup>

These require lower concentrations of applied CA, thus minimizing the risk of any  $\text{Gd}^{3+}$  intoxication. To achieve this goal, the key factors for MRI signal improvement have to be optimized. These factors include the rotational correlation time, the number of water molecules in the inner-sphere of the  $\text{Gd}^{3+}$  complex, their residence lifetime and the formation of the secondary hydration sphere.<sup>[13]</sup> It has been shown that the replacement of carboxylic groups in the aminocarboxylates with phosphonate groups leads to an increase in relaxivity due to the generation of water molecules in a secondary hydration sphere of the complex and/or to the catalysis of the inner-sphere water exchange process.<sup>[13–17]</sup>

Following these principles, we have previously reported the synthesis and initial characterization of the paramagnetic  $\text{Ln}^{3+}$  complexes with the appended phosphonate group on the DO3A core and variable aliphatic chain linkers.<sup>[18]</sup> Variation in the coordination environment of the  $\text{Ln}^{3+}$  centre led to changes in the physicochemical properties of both  $\text{Gd}^{3+}$  and  $\text{Eu}^{3+}$  complexes as a function of pH, and the relaxivity changes observed in  $\text{Gd}^{3+}$  acid-containing complexes indicated their potential for use in MR imaging as pH-responsive agents.

[a] Physiology of Cognitive Processes, Max Planck Institute for Biological Cybernetics, Spemannstr. 38, 72076 Tübingen, Germany  
Fax: +49-7071-601-919  
E-mail: ilgar.mamedov@tuebingen.mpg.de  
goran.angelovski@tuebingen.mpg.de

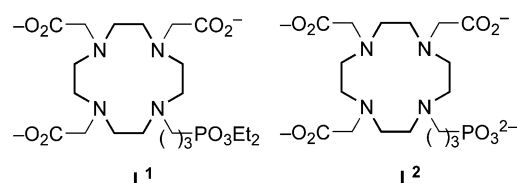
[b] Department of Chemistry, Masaryk University  
Kotlářská 2, 611 37 Brno, Czech Republic  
Fax: +420-549-49-2494  
E-mail: lubal@chemi.muni.cz

[c] Department of General, Organic and Biomedical Chemistry, NMR and Molecular Imaging Laboratory, University of Mons, Mons, Belgium

[d] Department for Inorganic Chemistry, Eberhard-Karls-Universität Tübingen, Tübingen, Germany

[e] Imaging Science and Biomedical Engineering, University of Manchester, Manchester, United Kingdom

In this work we report further physicochemical investigations of  $\text{Gd}^{3+}$  and  $\text{Eu}^{3+}$  complexes of  $\text{L}^1$  and  $\text{L}^2$  (Scheme 1), both containing a phosphonate group attached to the DO3A unit via the propyl linker. The relaxometric properties of  $\text{GdL}^1$  and  $\text{GdL}^2$  were investigated at various magnetic fields and temperatures. Potentiometric and NMR titrations with ligands  $\text{L}^1$  and  $\text{L}^2$ , as well as with  $\text{GdL}^1$  and  $\text{GdL}^2$ , were performed in order to determine protonation and stability constants. Finally, luminescence emission spectra of  $\text{EuL}^1$  and  $\text{EuL}^2$  were recorded in various conditions in order to characterize the thermodynamic and kinetic stability of these complexes and explore their potential for in vivo applications.



Scheme 1.

## Results and Discussion

### Relaxometric Experiments

Current MRI scanners used in clinical imaging operate at magnetic fields between 0.2–3 T. Therefore, we studied the paramagnetic properties of the  $\text{Gd}^{3+}$  complexes at body temperature (37 °C) with proton Larmor frequencies of 20 and 60 MHz, which correspond to magnetic fields of 0.47 T and 1.5 T, respectively. Proton relaxivity, defined as the increase in the proton relaxation rate induced by one millimole per litre of contrast agent, reflects the efficacy of MRI contrast agents.

As expected, both complexes exhibited higher longitudinal relaxivity values ( $r_1$ ) compared to the commercially available Dotarem® ( $\text{Gd-DOTA}$ , Table 1). In addition, the  $r_1$  of  $\text{GdL}^2$  increased by 54% and 56% at 20 MHz and 60 MHz, respectively, following alteration of the pH to 4, which is comparable to analogous relaxivity changes previously observed at 300 MHz (7 T).<sup>[18]</sup>

Table 1. Calculated proton longitudinal relaxivities ( $\text{mM}^{-1}\text{s}^{-1}$ ) at 20 MHz and 60 MHz, 37 °C.

Samples	20 MHz	60 MHz
$\text{GdL}^1$ , pH = 4	6.28	5.81
$\text{GdL}^1$ , pH = 7	5.89	5.47
$\text{GdL}^2$ , pH = 4	6.54	6.15
$\text{GdL}^2$ , pH = 7	4.26	3.94
$\text{Gd-DO3A}^{[a]}$ , pH = 7	4.80	—
$\text{Gd-DOTA}^{[b]}$ , pH = 7	3.50	3.10

[a] Ref.<sup>[19]</sup> [b] Ref.<sup>[20]</sup>

A different behaviour was obtained in the case of the ester-protected  $\text{GdL}^1$ , for which only slight changes in  $T_1$  relaxivity were observed in whole range of pH from 4 to 7.

Relaxivity arises mainly from the contributions of short-distance interactions between the paramagnetic ion and the coordinated water molecule(s) exchanging with the bulk, the so-called inner-sphere interaction, and from the long-distance interactions related to the diffusion of water molecules near the paramagnetic centre, the outer-sphere interaction. The first contribution is proportional to the number of water molecules in the first coordination sphere and can be limited by the water residence time. As already reported, the analogous  $\text{EuL}^1$  complex was shown to have two coordinated water molecules at both pHs studied, whereas  $\text{EuL}^2$  has a  $q$  value of 1.2 at pH 7 and 1.95 at pH 4.<sup>[18]</sup>

Along these lines, the increase in relaxivity observed for the  $\text{GdL}^2$  complex in acidic solution can thus be explained by an increase in the number of coordinated water molecules. The possible limitation of the relaxivity by the water residence time can easily be detected by the qualitative analysis of the proton relaxivity at 20 MHz on decreasing the temperature (Figure 1). Indeed, when reducing the temperature, the outer-sphere contribution increases while the inner-sphere contribution can either increase if the water residence time ( $\tau_M$ ) is smaller than the relaxation time of the hydrogen nuclei of this bound water molecule(s) ( $T_{1M}$ ), or decrease if  $\tau_M$  is larger than  $T_{1M}$ . The relaxivity of both complexes shows an exponential increase as temperature decreases.

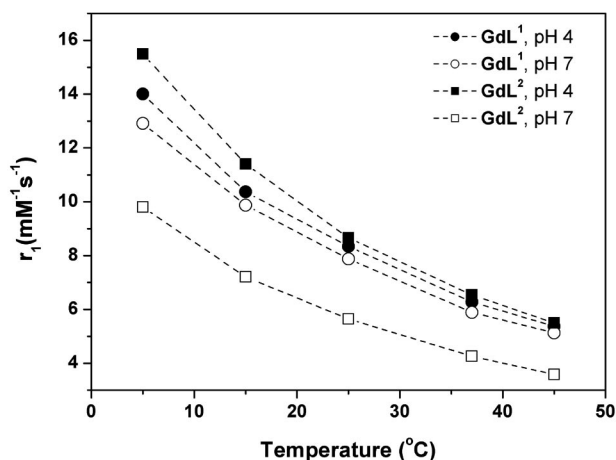


Figure 1. Proton longitudinal relaxivity studies at 20 MHz of  $\text{GdL}^1$  and  $\text{GdL}^2$  as a function of pH and temperature.

This behaviour indicates that the exchange rate does not limit relaxivity even at the lower temperatures. To further support these observations, the proton NMRD profiles of  $\text{GdL}^1$  and  $\text{GdL}^2$  were recorded at 37 °C (Figure 2). The NMRD curves were fitted according to the classical inner-sphere and outer-sphere theories.<sup>[21–23]</sup> Parameters obtained by the theoretical adjustment of the NMRD profiles are summarized in Table 2.<sup>[24]</sup> According to the data obtained in Figure 1, the  $\tau_M^{310}$  value was fixed to 100 ns, a value which is close to that of  $\text{Gd-DOTA}$  and has no effect on the relaxivity at 310 K.<sup>[20]</sup>

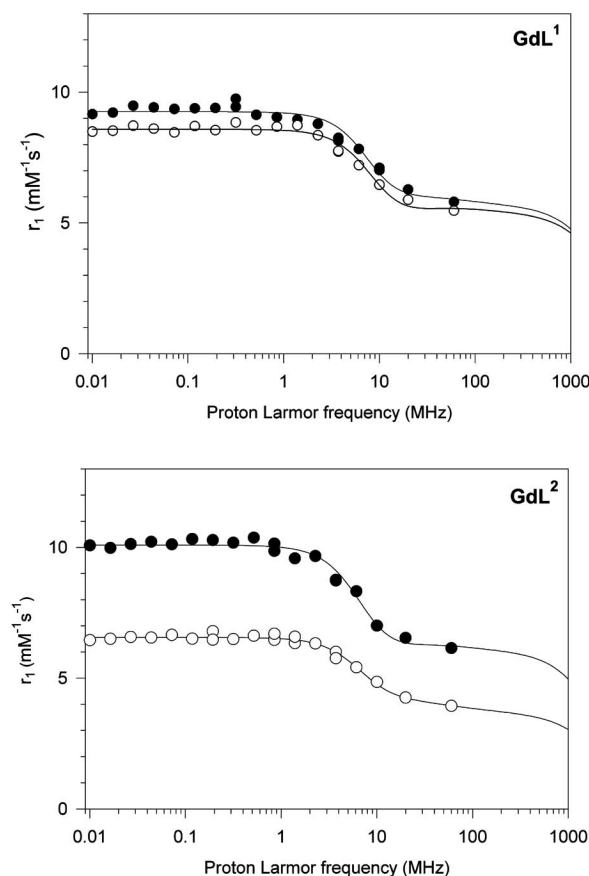


Figure 2. NMRD profiles of **GdL<sup>1</sup>** and **GdL<sup>2</sup>** at pH 4 (●) and pH 7 (○).

Table 2. Parameters obtained from the theoretical fitting of the NMRD data at 37 °C.<sup>[a]</sup>

	<b>GdL<sup>1</sup></b> pH 4	<b>GdL<sup>1</sup></b> pH 7	<b>GdL<sup>2</sup></b> pH 4	<b>GdL<sup>2</sup></b> pH 7	<b>GdDOTA</b> <sup>[b]</sup>
$\tau_R$ (ps)	$70.7 \pm 2.0$	$66.4 \pm 2.2$	$76.5 \pm 2.3$	$77.6 \pm 3.0$	$53 \pm 13$
$\tau_{SO}$ (ps)	$57.9 \pm 1.3$	$51.4 \pm 1.2$	$66.1 \pm 1.6$	$68.5 \pm 1.8$	$404 \pm 24$
$\tau_V$ (ps)	$16.5 \pm 1.1$	$13.2 \pm 0.9$	$15.2 \pm 1.2$	$15.9 \pm 1.5$	$7 \pm 1$
$q$	2	2	2	1	1

[a] Fixed parameters:  $q = 2$  for **GdL<sup>1</sup>** at both pHs and **GdL<sup>2</sup>** at pH 4,  $q = 1$  for **GdL<sup>2</sup>** at pH 7;  $d = 0.36$  nm,  $D = 3.3 \cdot 10^{-9}$  m<sup>2</sup> s<sup>-1</sup>,  $r = 0.31$  nm. [b] Ref.<sup>[20]</sup>

The values of the rotational correlation time ( $\tau_R$ ) of **GdL<sup>1</sup>** and **GdL<sup>2</sup>** were slightly enhanced compared to Gd-DOTA because of the slight increase in molecular size. The parameters characterizing the electronic relaxation rate (the electronic relaxation time at zero field  $\tau_{SO}$  and the correlation modulating the electronic relaxation time  $\tau_V$ ) were similar for both complexes. The lower value of  $\tau_{SO}$  of **GdL<sup>1</sup>** and **GdL<sup>2</sup>** compared to Gd-DOTA can be related to the decreased symmetry and/or rigidity of the complexes. Such an effect has previously been reported for Gd-DO3A.<sup>[19]</sup>

## pH-Potentiometric and NMR Studies

The protonation constants and complexing properties of the ligands **L<sup>1</sup>** and **L<sup>2</sup>** and their Gd<sup>3+</sup> complexes were studied by means of potentiometric and NMR titrations. The results obtained were compared with published data for other DO3A-based ligands, and the effect of the pendant arm on the protonation constants and complexing properties of the new macrocyclic ligands was studied.

**Determination of protonation constants.** The protonation constants of macrocyclic ligands were determined at 25 °C and ionic strength of 0.1 M (NaCl). This supporting electrolyte was chosen as such experimental conditions are close to the in vivo environment and overcome problems with determination of the highest protonation constants. In addition, after obtaining the stability constants of the sodium complex with the studied ligands, the values of conditional protonation constants for constant sodium ion concentration could be calculated for comparison to indirectly confirm the reliability of the obtained values.

The protonation constants of ligands **L<sup>1</sup>** and **L<sup>2</sup>** are given in Table 3 and the values for analogous ligands (DO3A, DOTA and DO3AMP) are also presented for comparison. Since the structural changes in the macrocyclic ligands were not as dramatic, it was expected that the protonation scheme would be comparable for all DO3A-like derivatives. The reverse order of  $\log K_{p,1}$  and  $\log K_{p,2}$  for **L<sup>1</sup>** likely means that protons are binding to nitrogen atoms in the macrocyclic cavity almost simultaneously and are not influenced by the pendant arm.<sup>[25]</sup> The protonation constant of the phosphonate group in **L<sup>2</sup>** is apparently dependent on the chain length of the pendant arm and is similar to the protonation constant of methylphosphonic acid ( $\log K_p = 7.54$ ,  $I = 0.1$  M NaNO<sub>3</sub>,  $t = 25$  °C).<sup>[29]</sup> A similar effect was observed for the decrease in basicity of the nitrogen ring atom (see  $\log K_{p,2}$ ) with prolongation of the pendant group which is closer to 9.72 for DOTA where no hydrogen bonding is assumed. These two protonation constants obtained by glass-electrode potentiometry were also verified by NMR spectroscopy (Table 3 and Figure 3). The values obtained by both experimental techniques are in rough agreement. Other values were hard to obtain due to broad <sup>1</sup>H NMR spectra and complicated assignment of particular proton resonances. However, the increase of  $\log K_{p,3}$  in **L<sup>2</sup>** compared to the analogous value in DO3AMP is probably related to weakening of the hydrogen bond with the prolongation of chain length, resulting in the phosphonate group being less acidic. Moreover, it remains possible that the phosphonate group interacts with other acetate arms.

In the case of **L<sup>1</sup>**, in which the phosphonate pendant arm is protected in the form of bis(esters), lower values were found for protonation constants of nitrogen atoms in the cyclen ring and these were much closer to values found for the DOTA ligand, compared to the protonation constants obtained for macrocyclic ligands that contain a free phosphonate group (DO3AMP, **L<sup>2</sup>**). This sharp decrease in basicity has been observed previously and also reported for other macrocyclic ligands containing ester groups.<sup>[30]</sup>

Table 3. Logarithmic values of protonation constants of studied macrocyclic ligands,<sup>[a]</sup>  $t = 25\text{ }^{\circ}\text{C}$ ,  $I = 0.1\text{ M NaCl}$  (otherwise the medium is mentioned). The values are defined as  $K_{p,i} = [\text{H}_i\text{L}][\text{H}^+]^{-1}[\text{H}_{i-1}\text{L}]^{-1}$  and  $\log\beta_{p,i} = \sum \log K_{p,i}$ .

Ligand	$\log K_{p,1}$	$\log K_{p,2}$	$\log K_{p,3}$	$\log K_{p,4}$	$\log K_{p,5}$	$\sum \log K_{p,i} (n = 4)$
DO3A	11.19	9.48	4.21	3.35	—	28.23
DO3A <sup>[b]</sup>	12.46 (11.24 <sup>[c]</sup> )	9.49	4.26	3.51	1.97	29.72 (28.50 <sup>[c]</sup> )
DOTA <sup>[d]</sup>	11.9 (8.70 <sup>[c]</sup> )	9.72	4.60	4.13	2.36	30.35 (27.15 <sup>[c]</sup> )
DO3AMP <sup>[e]</sup>	13.83 (10.05 <sup>[c]</sup> )	10.35	6.54	4.34	3.09	34.37 (27.83 <sup>[c,f]</sup> )
<b>L<sup>1</sup></b>	9.37	9.45	4.13	2.94 <sup>[g]</sup>	—	25.89
<b>L<sup>2</sup></b>	11.09	9.94 (9.78 <sup>[h]</sup> )	7.17 (6.84 <sup>[h]</sup> )	4.00	2.82	35.02 (27.85 <sup>[f]</sup> )

[a] For  $\log K_{p,i}$  the standard deviation is  $\leq 0.04\text{ log }K$  unit. [b] TMACl, Ref.<sup>[26]</sup> [c] Measured at  $I = 0.1\text{ M}$  TMACl, corrected for sodium ion complexation ( $\log K_{\text{Na}} = 2.2 - \text{DO3A}$ ,  $4.03 - \text{DOTA}$ ,  $4.77 - \text{DO3AMP}$ ). [d] TMACl, Ref.<sup>[26,28]</sup> [e] DO3AMP = DO3A-methylphosphonate, Ref.<sup>[27,28]</sup> [f] The overall protonation constant calculated without the protonation constant of the phosphonic pendant arm. [g] Estimated value. [h]  $\log K_{p,7} \approx 1.5$  measured by  $^{31}\text{P}$  and  $^1\text{H}$  NMR spectroscopy without control of the ionic strength.

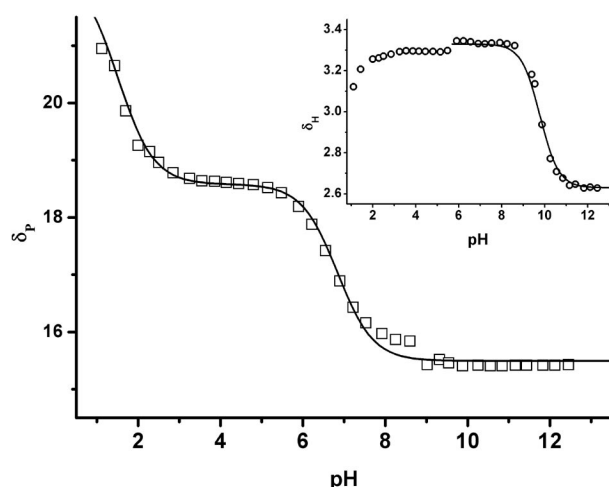


Figure 3.  $\delta_P$  and  $\delta_H$  (inset) of methylene protons neighbouring the nitrogen of the **L<sup>2</sup>** phosphonate pendant arm as a function of pH. The experimental points were fitted with parameters:  $\log K_p(-\text{PO}_3^{2-}) = 6.84 \pm 0.05$ ,  $\log K_p(-\text{HPO}_3^-) = 1.5 \pm 0.1$ ,  $\delta_{\text{H}2\text{L}} = 20.9$  (estimate),  $\delta_{\text{HL}} = 18.58$ ,  $\delta_{\text{L}} = 15.50$  ( $^{31}\text{P}$  NMR spectroscopy),  $\log K_p(-\text{N}(\text{CH}_2)_3\text{PO}_3^{2-}) = 9.78 \pm 0.1$ ,  $\delta(-\text{NCH}_2-) = 2.63$ ,  $\delta(-^+\text{HNCH}_2-) = 3.33$ .

The potentiometric titrations were also performed with **GdL<sup>1</sup>** and **GdL<sup>2</sup>** and their protonation constants were determined (Table 4, values for Gd-DO3AMP are given for comparison). The ester-protected **GdL<sup>1</sup>** has only one protonation constant ( $\log K = -11.1$ ), which can be attributed to deprotonation of the inner-sphere bound water molecule. The protonation constant of the inner-sphere water molecule in **GdL<sup>2</sup>** is similar ( $\log K = -11.4$ ), whereas the phosphonate group is more acidic as in the case of the free ligand **L<sup>2</sup>** ( $\log K = 5.2$ ). The obtained value actually matches the region in which the most dramatic relaxivity change of **GdL<sup>2</sup>** occurs, confirming that the (de)protonation of the

phosphonate group is the process that is most responsible for the observed changes. In addition, the protonation constants for the **GdL<sup>2</sup>** complex are consistent with the dependence of relaxivity on pH.<sup>[18]</sup>

**Determination of stability constants of  $\text{Ca}^{2+}$  complexes.** The stability constants of  $\text{Gd}^{3+}$  complexes found in the literature vary for different experimental conditions (mostly pH, type of supporting electrolyte, temperature, etc.) and experimental techniques.<sup>[31]</sup> However, their determination by potentiometry is challenging because of the slow complex formation, and thus some additional adjustments to the methods, such as “out of cell” titrations, are commonly used.<sup>[27]</sup> On the other hand, the complexation reaction with metals such as  $\text{Ca}^{2+}$  is fast enough to determine equilibrium constants by means of potentiometric titration using the glass ion-selective electrode. Finally, the stability constants of  $\text{Ca}^{2+}$  complexes thus obtained can be used for the possible estimation of the stability constants of complexes with  $\text{Ln}^{3+}$  ions (e.g.  $\text{Gd}^{3+}$  complexes).

The potentiometric titrations of **L<sup>1</sup>** and **L<sup>2</sup>** in the presence of  $\text{Ca}^{2+}$  were performed at  $25\text{ }^{\circ}\text{C}$  and  $I = 0.1\text{ M}$  (NaCl). The results are summarized in Table 5 and compared with analogous values for DO3A, DOTA and DO3AMP. The order of stability of  $\text{Ca}^{2+}$  complexes is the following: DO3AMP (17.38)  $\approx$  DOTA (17.22)  $>$  **L<sup>2</sup>** (11.99)  $\approx$  DO3A (11.96)  $>$  **L<sup>1</sup>** (10.13). Notably, the highest stability of all  $\text{Ca}^{2+}$  complexes occurs in DO3AMP and the stability of the complex is comparable with DOTA. This result was expected as both complexes possess a coordination number of eight (CN 8), compared to the DO3A type with a CN of seven, which exhibits lower stability with  $\text{Ca}^{2+}$ . The phosphonate group of **L<sup>2</sup>**, being more distant from the macrocyclic cavity as compared to DO3AMP, apparently does not influence the complex stability of **CaL<sup>2</sup>**, which is indeed similar to the stability of  $\text{Ca-DO3A}$ . Despite the influence on the number of inner-sphere water molecules and thus the relaxivity in **GdL<sup>2</sup>**, one could note that existence of the pH sensitivity in this complex speaks for rather weak interaction of phosphonates with the ion in the macrocyclic cavity which does not contribute to the stability of the complex. DO3AMP analogues however exhibit no sensitivity to pH changes and higher values obtained for stability constants are in line with a stronger coordination of phosphonate with the metal ion.<sup>[33]</sup>

Table 4. Logarithmic values of protonation constants of studied complexes,  $t = 25\text{ }^{\circ}\text{C}$ ,  $I = 0.1\text{ M NaCl}$ .

Reaction	DO3AMP <sup>[a]</sup>	<b>L<sup>1</sup></b>	<b>L<sup>2</sup></b>
$\text{GdL} + \text{H} \rightarrow \text{Gd(HL)}$	5.42	—	5.2
$\text{GdL(H}_2\text{O)} \rightarrow \text{GdL(OH)} + \text{H}$	−12.72	−11.1	−11.4

[a] Ref.<sup>[27]</sup>



Table 5. Logarithmic values of stability constants of complex formation with studied macrocyclic ligands,  $t = 25\text{ }^{\circ}\text{C}$ ,  $I = 0.1\text{ M NaCl}$  (otherwise the medium is mentioned).<sup>[a]</sup>

Reaction <sup>[b]</sup>	DO3A		DOTA	DO3AMP	L <sup>1</sup>	L <sup>2</sup>
Ca + L → CaL	11.96	13.39 <sup>[c]</sup> (12.16 <sup>[d]</sup> )	17.22 <sup>[c]</sup> (14.19 <sup>[d]</sup> )	17.38 <sup>[c]</sup> (13.27 <sup>[d]</sup> )	10.13	11.99
Ca + L + H → Ca(HL)	17.47	—	—	24.87 <sup>[c]</sup> (21.10 <sup>[d]</sup> )	14.8 <sup>[f]</sup>	19.68
Ca + L + 2H → Ca(H <sub>2</sub> L)	22.82	—	—	29.05 <sup>[c]</sup> (25.28 <sup>[d]</sup> )	—	25.71
Ca + L + 3H → Ca(H <sub>3</sub> L)	—	—	—	32.16 <sup>[c]</sup> (28.39 <sup>[d]</sup> )	—	30.97
CaL + H → Ca(HL)	5.51	—	3.80 <sup>[c]</sup>	7.83	4.7 <sup>[f]</sup>	7.69
Ca(HL) + H → Ca(H <sub>2</sub> L)	5.35	—	3.77 <sup>[c]</sup>	4.18	—	6.03
CaL + 2H → Ca(H <sub>2</sub> L)	10.86	11.36 <sup>[c]</sup>	7.57 <sup>[c]</sup>	12.01	—	—
Ca(H <sub>2</sub> L) + H → Ca(H <sub>3</sub> L)	—	3.8 <sup>[c]</sup>	—	3.11	—	5.26
Ca + HL → Ca(HL)	6.28	—	9.28	10.75	5.41	8.59
Ca + H <sub>2</sub> L → Ca(H <sub>2</sub> L)	2.15	2.79	3.29	8.39	—	4.67
Ca + H <sub>3</sub> L → Ca(H <sub>3</sub> L)	—	2.33	—	7.16	—	2.76
CaL + OH → CaL(OH)	—	—	—	—	−11.6	—

[a] For  $\log K$  the standard deviation is  $\leq 0.04 \log K$  unit. [b] The charges are omitted for the sake of clarity. [c] Ref.<sup>[26]</sup> [d] Corrected for sodium ion concentration (see values in Table 3). [e] Ref.<sup>[32]</sup> [f] Estimated value.

Because of the linear correlation existing between stability values of  $\text{Ca}^{2+}$  and  $\text{Gd}^{3+}$  complexes, the abovementioned formula [Equation (1)] was used to estimate the stability constants of  $\text{Gd}^{3+}$  complexes based on the calculated values obtained for  $\text{Ca}^{2+}$  complexes.<sup>[34]</sup> The following stability constants of  $\text{Gd}^{3+}$  complexes were calculated: 22.4 (DOTA), 21.1 (DO3AMP), 19.2 (DO3A), 19.3 (L<sup>2</sup>), 16.7 (L<sup>1</sup>), suggesting that the thermodynamic stability of  $\text{GdL}^2$  is sufficient for potential in vivo application.

$$\log K_{\text{GdL}} = (1.4 \pm 0.1) \times \log K_{\text{CaL}} + (2.5 \pm 1.2) \quad (1)$$

## Luminescence Studies

**Determination of the stability constants.** The stability constants of  $\text{EuL}^1$  and  $\text{EuL}^2$  were studied by means of luminescence spectroscopy. The luminescence intensity of equilibrated solutions of EuL complexes at different pHs was measured in order to eliminate formation of  $\text{Ln}_2\text{L}$  complexes (Figure 4). The conditional stability constants  $\log \beta_{\text{cond}}$  were corrected for the side chemical equilibria, e.g. ligand and  $\text{Eu}^{3+}$  complex protonation,  $\text{Eu}^{3+}$ -formate complexation, etc. The calculated values for the stability con-

stants were  $16.0_8 \pm 0.1_4$  and  $19.5_8 \pm 0.1_7$  for  $\text{EuL}^1$  and  $\text{EuL}^2$ , respectively. These values correspond well to the stability constants estimated for  $\text{Gd}^{3+}$  complexes using Equation (1) (see determination of stability constants of  $\text{Ca}^{2+}$  complexes) given the small and expected differences in the stability of  $\text{Gd}^{3+}$  and  $\text{Eu}^{3+}$  complexes.<sup>[35]</sup>

However, this methodology proved to be reliable and useful in the determination of the stability constant estimates of  $\text{Ln}^{3+}$  complexes, mainly  $\text{Eu}^{3+}$  and  $\text{Gd}^{3+}$ . On the basis of values determined for all equilibrium constants, the simulation of distribution diagrams of  $\text{EuL}^2$  as a function of solution acidity was performed (Figure 5).

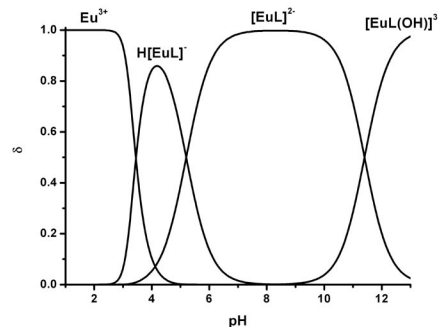


Figure 5. The distribution diagram calculated from the protonation and stability constants for  $\text{EuL}^2$ .

**Formation kinetics.** Studies of the formation kinetics of complexes  $\text{EuL}^1$  and  $\text{EuL}^2$  were performed in slightly acidic media (pH 4.9–5.6) in which the formation of complexes is nearly complete (Figure 5) although it is still sufficiently slow to be followed by conventional molecular spectroscopy. The rate of complex formation between the  $\text{Eu}^{3+}$  ion and the ligand can be written as a second-order rate law [Equation (2)].

$$v = k_2 \times [\text{L}]_{\text{tot}} \times [\text{Eu}^{3+}]_{\text{tot}} \quad (2)$$

The second-order rate constants are dependent on proton concentration [Equation (3)], where the denominator  $a_L$  is calculated according to Equation (4), using the ligand protonation constants  $\beta_{p,n}$  as defined in the potentiometric section.

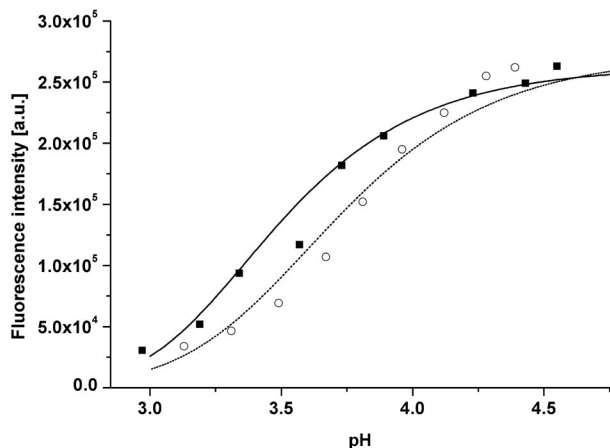


Figure 4. The pH dependence of fluorescence intensity of  $\text{EuL}^1$  (■) and  $\text{EuL}^2$  (○) ( $c_{\text{Eu}} = c_{\text{L}} = 6.0\text{ mM}$ ,  $\lambda_{\text{ex}} = 394\text{ nm}$ ,  $\lambda_{\text{em}} = 616\text{ nm}$ ).

$$^f k_2 = \frac{\sum_{i=0}^n {}^f k_{\text{H}_i\text{L}} \times \beta_i \times [\text{H}^+]^i}{\alpha_{\text{L}}} \quad (3)$$

$$\alpha_{\text{L}} = \beta_{p,5} \times [\text{H}^+]^5 + \beta_{p,4} \times [\text{H}^+]^4 + \beta_{p,3} \times [\text{H}^+]^3 + \beta_{p,2} \times [\text{H}^+]^2 + \beta_{p,1} \times [\text{H}^+] + 1 \quad (4)$$

The rate constants  $^f k_2$  were fitted as a function of solution acidity (see Figure 6) according to Equation (3), and the obtained rate constants are shown in Table 6. As can be seen for the **L**<sup>2</sup> ligand, the less protonated species are more reactive than the more protonated ones. The reaction mechanism of Eu<sup>3+</sup> with the abovementioned protonated species in the case of DO3AMP has already been postulated.<sup>[28]</sup>

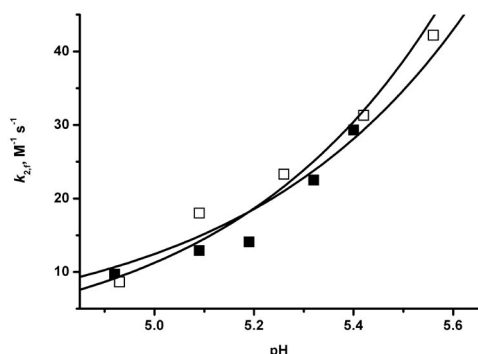


Figure 6. The dependence of the second-order rate constant  $^f k_2$  on pH for formation of **EuL**<sup>1</sup> (□) and **EuL**<sup>2</sup> (■).

Table 6. Formation rate constants of **EuL**<sup>1</sup> and **EuL**<sup>2</sup>.

Complex	Rate constant [M <sup>-1</sup> s <sup>-1</sup> ]
<b>EuL</b> <sup>1</sup>	$^f k(\text{HL}) = 3.73 \pm 0.27 \times 10^5$
<b>EuL</b> <sup>2</sup>	$^f k(\text{H}_3\text{L}) = 4.2 \pm 1.3$ , $^f k(\text{H}_2\text{L}) = (1.18 \pm 0.18) \times 10^3$

In order to compare the experimental data presented here with that found in the literature, the  $k_{\text{f,obs}}$  values of pseudo-first order were calculated as  $k_{\text{f,obs}} = ^f k_2 \times [\text{L}]_{\text{tot}}$  since the formation kinetics were studied in excess of ligand with respect to Eu<sup>3+</sup>. The obtained values were fitted as a function of [OH<sup>-</sup>] (Figure 7). The dependence was linear with no intercept observed. A similar case was observed for EuDO3AMP. Also, the calculated values  $k_{\text{OH}} = (3.15 \pm 0.15) \times 10^6 \text{ M}^{-1} \text{ s}^{-1}$  and  $(3.47 \pm 0.12) \times 10^6 \text{ M}^{-1} \text{ s}^{-1}$  for **EuL**<sup>1</sup> and **EuL**<sup>2</sup>, respectively, are roughly in agreement with the value  $(2.7 \pm 0.2) \times 10^6 \text{ M}^{-1} \text{ s}^{-1}$  obtained for EuDO3AMP.<sup>[28]</sup> On the basis of the absence of any dramatic difference in the pseudo-first-order rate constants between all studied phosphonate-containing ligands (DO3AMP, **L**<sup>1</sup>, **L**<sup>2</sup>), one could conclude that the prolongation of the side arm does not have any notable influence on the formation kinetics. In addition, no effect of the ester substitution on the phosphonate pendant arm was observed.

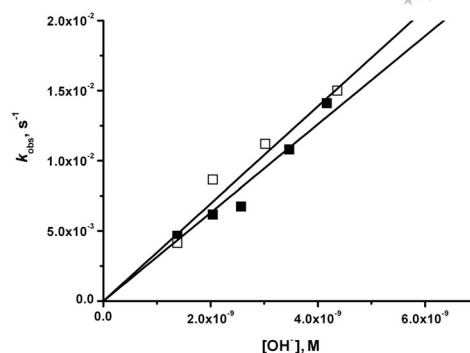


Figure 7. The dependence of the pseudo-first-order rate constant  $k_{\text{f,obs}}$  on [OH<sup>-</sup>] concentration for formation of **EuL**<sup>1</sup> (□) and **EuL**<sup>2</sup> (■).

**Dissociation kinetics.** The acid-assisted dissociation reaction of **EuL**<sup>1</sup> and **EuL**<sup>2</sup> was studied in order to estimate the kinetic inertness of the Ln<sup>3+</sup> complexes with the macrocyclic ligands. The proton-assisted dissociation kinetics experiments were performed in the presence of strong mineral acids ( $c = 0.5\text{--}3.0 \text{ M}$ ) since the Ln<sup>3+</sup> complexes are thermodynamically unstable under these experimental conditions (see Figure 5). The mechanism for dissociation of the Ln<sup>3+</sup> complex with the analogous type of ligands (DO3AMP) has already been established.<sup>[27,28]</sup> Assuming that the [Eu(H<sub>3</sub>L)]\* complex species take part in the dissociation process, the rate of dissociation of the Eu<sup>3+</sup> complexes is defined as in Equation (5), where the respective protonation constants of the Eu<sup>3+</sup> complex are generally defined as in Equation (6).

$$-\frac{d[\text{complex}]}{dt} = k_{\text{Eu}(\text{H}_2\text{L})} \times [\text{Eu}(\text{H}_2\text{L})] + k_{\text{Eu}(\text{H}_3\text{L})} \times [\text{Eu}(\text{H}_3\text{L})] \quad (5)$$

$$^{\text{H}} K_i = \frac{[\text{Eu}(\text{H}_i\text{L})]}{[\text{Eu}(\text{H}_{i-1}\text{L})] \times [\text{H}^+]} \quad (6)$$

Combining the mass-balance equation with the relationships given above and then simplifying it gives Equation (7).

$$^{\text{Eu}} k_{\text{d,obs}} = \frac{k_{\text{Eu}(\text{H}_3\text{L})} \times ^{\text{H}} K_3 \times [\text{H}^+]}{1 + ^{\text{H}} K_3 \times [\text{H}^+]} \quad (7)$$

Finally, when  $^{\text{H}} K_3$  is very low, the simplified Equation (8) can be used to calculate the rate constants.

$$^{\text{Eu}} k_{\text{d,obs}} \approx k_{\text{Eu}(\text{H}_3\text{L})} \times ^{\text{H}} K_3 \times [\text{H}^+] = k_{\text{H}} \times [\text{H}^+] \quad (8)$$

The kinetics of the proton-assisted decomplexation of **EuL**<sup>1</sup> and **EuL**<sup>2</sup> were studied (Figure 8) and Equation (8) was employed in order to fit the experimental points. The dissociation rate constants were calculated as  $k_{\text{H}} = (1.16 \pm 0.03) \times 10^{-4} \text{ M}^{-1} \text{ s}^{-1}$  and  $k_{\text{H}} = (1.18 \pm 0.02) \times 10^{-4} \text{ M}^{-1} \text{ s}^{-1}$  for **EuL**<sup>1</sup> and **EuL**<sup>2</sup>, respectively. As can be seen, the experimental points for both complexes fall together and thus the obtained parameters are almost identical within experimental error. The values are similar to those

previously described for the dissociation of other analogous complexes: EuDO3AMP ( $k_H = 0.98 \times 10^{-5} \text{ M}^{-1} \text{ s}^{-1}$ ), and EuDO3A-methylphosphinic acid propionate ( $k_H = 1.03 \times 10^{-4} \text{ M}^{-1} \text{ s}^{-1}$ ).<sup>[27]</sup> On the basis of the obtained constants, the half-time of  $\text{Eu}^{3+}$  complex decomposition at  $\text{pH} \approx 2$  is about 6.8–6.9 h, which is comparable with the value 7.9 h obtained for the  $\text{Gd}^{\text{III}}$  complex with DO3AMP.<sup>[27]</sup> This time can be accelerated in the presence of some biometal ions or bioligands. However, it should be considered as sufficient for the potential application of the contrast agent given that such extreme conditions are not present in vivo.

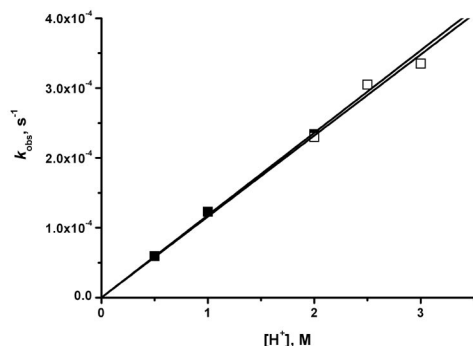


Figure 8. The dependence of the pseudo-first-order rate constant  $k_{d,obs}$  on  $[\text{H}^+]$  concentration for the acid-assisted dissociation of  $\text{EuL}^1$  (□) and  $\text{EuL}^2$  (■).

## Conclusions

Two DO3A-based ligands and their  $\text{Gd}^{3+}$  and  $\text{Eu}^{3+}$  complexes containing ethyl-protected and unprotected propylphosphonates in the side chain were investigated. Relaxometric studies of the acid-containing  $\text{Gd}^{3+}$  complex at 20 and 60 MHz showed that longitudinal relaxivity increases when the pH of the medium changes from neutral to slightly acidic (pH 4). Such changes were not observed in the case of the ester-protected  $\text{Gd}^{3+}$  complex as the  $r_1$  remains constant in the studied pH range. The temperature-dependent relaxivity measurements demonstrated fast water exchange for both complexes. Investigations of the magnetic properties of the complexes as a function of the magnetic field strength and the comparison of the data with the DO3A and DOTA complexes excluded the possibility of oligomerization processes in the investigated systems, which sometimes take place in the phosphonate-containing chelates. The protonation constants of the ligands are similar to DO3A-type molecules. The increased distance from the macrocyclic ring of the propylphosphonate in comparison to the methylphosphonate leads to the decreased acidity of the phosphonic group and decreased basicity of the nitrogen on the ring. The calculated protonation constant of the phosphonate in the  $\text{Gd}^{3+}$  complex is exactly in the pH range in which the highest relaxivity changes occur. Studies on the formation kinetics of the  $\text{Eu}^{3+}$  complexes indicated that neither ester-protected nor unprotected propylphosphonate groups have a notable influence on the rate of complex formation. The thermodynamic properties of the com-

plexes were studied via two independent methods, namely using potentiometric titrations for the determination of stability of  $\text{Gd}^{3+}$  complexes, and luminescence emission spectroscopy for the determination of the stability of  $\text{Eu}^{3+}$  complexes. The results obtained from the two methods are in the same range, suggesting that the values for the stability constants are sufficient and comparable to the thermodynamic values of commercial contrast agents used for in vivo imaging. In addition, dissociation kinetic studies suggest a very slow dissociation rate of the complexes even in very acidic conditions, supporting the possible in vivo application of these systems, especially the complex possessing “smart” properties, which could be used to report pH changes in living tissues.

## Experimental Section

**General:** The ligands used in this work were synthesized according to previously described procedures.<sup>[18]</sup> Stock solutions of ligands were prepared by dissolving a known amount in bi-distilled water. Lanthanide salts (*p.a.* quality) were supplied by Aldrich. All other chemicals such as NaOH, HCl, formic acid, and acetic acid were purchased from Merck and they were of the highest available purity. The stock solutions of  $\text{LnCl}_3$  were obtained by dissolving the solid in distilled water and then the precise concentrations were determined by chelatometric titration.<sup>[36]</sup>

Longitudinal relaxation rates  $R_1$  were measured with a Bruker Minispec mq 20 at 20 MHz (0.47 T), mq 60 at 60 MHz (1.5 T) and 37 °C. The concentration of each sample was determined by the following procedure: 150  $\mu\text{L}$  of solutions of complexes  $\text{GdL}^1$  and  $\text{GdL}^2$  and 150  $\mu\text{L}$  of  $\text{HNO}_3$  were mixed to induce decomplexation and the  $R_1$  of the resulting solution was measured. Since the relaxation rate for 1 mM solution of free  $\text{Gd}^{3+}$  is  $11.76 \text{ s}^{-1}$  in  $\text{HNO}_3$  solution, the  $\text{Gd}^{3+}$  concentration could be determined in this way. The NMRD curves were obtained with a Stelar fast field cycling relaxometer (PV, Mede, Italy). Fitting of the  $^1\text{H}$  NMRD profiles was performed with data-processing software that uses the theoretical models describing the nuclear relaxation phenomena observed (Minuit, CERN Library).<sup>[37,38]</sup>

The equilibrium constants (protonation constants, stability constants) for macrocyclic ligands of interest were determined at temperature  $25.0 \pm 0.3$  °C and ionic strength 0.1 M, adjusted by sodium chloride. The aqueous solutions of macrocyclic ligands or prepared metal complexes (determination of protonation constants) or their mixtures with calcium ions (usually ratio 1:1 for determination of stability constants) were titrated in a vessel by 0.1 M NaOH solution in  $-\log[\text{H}^+]$  range 2–12 where no correction for liquid junction potential was applied. An inert atmosphere was ensured by bubbling the titrated solution with argon. The potentiometric titrations were performed with a Metrohm 794 Basic Titrimo instrument with a combined glass electrode (METROHM) for determination of free proton concentration in solution. The measured experimental data were transferred via an RS 232C data interface onto a computer using Metrodata VESUV PC software and the experimental data were treated using OPIUM software in order to determine the equilibrium constants from titration curves.<sup>[39,40]</sup> The combined electrode was calibrated using the following calibration function:  $E = E_0 + S \log[\text{H}^+]$ , where  $E_0$  is the standard potential including mostly the contribution of the reference electrode, and  $S$  corresponds to the Nernstian slope, the value of which should be close to the theoretical value. The calibration parameters were estimated from ti-

tration of a diluted solution of the standard HCl with the standard 0.1 M NaOH solution. The concentration of the standard NaOH solution was checked against potassium hydrogen phthalate. The values of  $E_0$  were in the range 405–415 mV, while the slope  $S$  was about 58.5–59.8 mV  $(-\log[H^+])^{-1}$ , which is in agreement with the expected value for the Nernstian slope of a glass ion-selective electrode. The water ionic product was determined in order to check the correct functioning of our experimental instrumentation and was  $pK_w = 13.80 \pm 0.02$  (commonly accepted values  $13.78 \pm 0.01$  and  $13.79$ ).<sup>[41]</sup>

pH-NMR titration experiments were recorded with a Bruker Avance II 300 MHz 'Microbay' spectrometer at 25 °C. The pH of  $L^2$  (0.3 mM) in  $H_2O$  was adjusted with 0.1 M NaOH and measured with a pH-meter calibrated with standard buffers.

Luminescence emission spectroscopy experiments were performed with a QuantaMaster QM 3PH (PTI, United Kingdom) spectrometer. The  $Eu^{3+}$  complexes were excited at  $\lambda_{ex} = 394$  nm and the  $^5D_0 \rightarrow ^7F_2$  emission band was used for both kinetic (formation and dissociation) and thermodynamic (determination of stability constants of  $Eu^{3+}$  complex) studies. The ionic strength  $I = 0.1$  M in all experiments was adjusted by addition of NaCl. The formation kinetics experiments were carried out in acetate buffer ( $c_T \approx 0.42$  M, pH = 4.9 and 5.6), mixing  $EuCl_3$  and the ligand stock solutions in a cuvette ( $c_{Eu} = 1.9 \times 10^{-4}$  M,  $c_L = 4.8 \times 10^{-4}$  M). The emission intensity was measured at a fixed time interval (usually between 20 and 180 s). The dissociation kinetics experiments were started by mixing  $EuL$  ( $c = 5.0 \times 10^{-4}$  M) complex and HCl solution ( $c_{HCl} = 0.5$ – $3.0$  M) while keeping ionic strength constant by addition of sodium perchlorate ( $I = 3.0$  M). All kinetics data were evaluated using PRO-K II software.<sup>[42]</sup> The determination of stability constants of  $Eu^{3+}$  complexes was carried out by luminescence measurements and experimental data treatment as described in the literature.<sup>[35]</sup> In order to verify the calculated stability constants, OPIUM software was employed and the values obtained by both approaches were consistent. The  $EuCl_3$  and ligand stock solutions were mixed in a 1:1 ratio ( $c_{Eu} \approx c_L = 6.0 \times 10^{-3}$  M) in formate buffer ( $c_T \approx 0.36$  M, pH  $\approx 3$ ) and the pH solution was adjusted by adding small droplets of concentrated NaOH and HCl solutions. The prepared solutions were left for at least three days prior to the luminescence measurements in order to achieve equilibrium.

## Acknowledgments

The authors thank Prof. Robert N. Muller for helpful discussions during the preparation of the manuscript. Financial support from the Max Planck Society, the Hertie Foundation, the Louis Jeantet Foundation, Fonds National de la Recherche Scientifique (FNRS), the French Community of Belgium ARC (Concerted Research Action) and the European Union (EMIL Network of Excellency, FP6) is gratefully acknowledged. The work was carried out within the framework of COST Action D38.

- [1] R. B. Lauffer, *Chem. Rev.* **1987**, 87, 901–927.
- [2] A. E. Merbach, E. Toth (Eds.), *The Chemistry of Contrast Agents in Medical Magnetic Resonance Imaging*, John Wiley & Sons, New York, **2001**.
- [3] P. Caravan, J. J. Ellison, T. J. McMurry, R. B. Lauffer, *Chem. Rev.* **1999**, 99, 2293–2352.
- [4] S. M. Rocklage, A. D. Watson, *J. Magn. Reson. Imaging* **1993**, 3, 167–178.
- [5] G. Dorta, A. Uske, A. L. Blum, *Digestion* **1997**, 58, 289.
- [6] R. Delgado, V. Felix, L. M. P. Lima, D. W. Price, *Dalton Trans.* **2007**, 2734–2737.

- [7] I. Lukeš, J. Kotek, P. Vojtišek, P. Hermann, *Coord. Chem. Rev.* **2001**, 216, 287–305.
- [8] L. Burai, R. Király, I. Lázár, E. Brücher, *Eur. J. Inorg. Chem.* **2001**, 813–820.
- [9] P. Wedeking, K. Kumar, M. F. Tweedle, *Magn. Reson. Imaging* **1992**, 10, 641–648.
- [10] E. Brücher, *Top. Curr. Chem.* **2002**, 221, 103–122.
- [11] L. Helm, *Prog. Nuc. Mag. Res. Spec.* **2006**, 49, 45–64.
- [12] J. B. Livramento, E. Toth, A. Sour, A. Borel, A. E. Merbach, R. Ruloff, *Angew. Chem. Int. Ed.* **2005**, 44, 1480–1484.
- [13] Z. Kotková, G. A. Pereira, K. Djanashvili, J. Kotek, J. Rudovský, P. Hermann, L. Vander Elst, R. N. Muller, C. F. G. C. Geraldes, I. Lukeš, J. A. Peters, *Eur. J. Inorg. Chem.* **2009**, 119–136.
- [14] P. Hermann, J. Kotek, V. Kubiček, I. Lukeš, *Dalton Trans.* **2008**, 3027–3047.
- [15] S. Aime, E. Gianolio, D. Corpillo, C. Cavallotti, G. Palmisano, M. Sisti, G. B. Giovenzana, R. Pagliarin, *Helv. Chim. Acta* **2003**, 86, 615–632.
- [16] P. Lebduškova, P. Hermann, L. Helm, É. Tóth, J. Kotek, K. Binnemans, J. Rudovský, I. Lukeš, A. E. Merbach, *Dalton Trans.* **2007**, 493–501.
- [17] S. Zhang, K. Wu, A. D. Sherry, *Angew. Chem. Int. Ed.* **1999**, 38, 3192–3194.
- [18] I. Mamedov, A. Mishra, G. Angelovski, H. A. Mayer, L.-O. Pålsson, D. Parker, N. K. Logothetis, *Dalton Trans.* **2007**, 5260–5267.
- [19] S. Aime, M. Botta, S. Geninatti Crich, G. Giovenzana, R. Pagliarin, M. Sisti, E. Terreno, *Magn. Reson. Chem.* **1998**, 36, S200–S208.
- [20] S. Laurent, L. Vander Elst, R. N. Muller, *Contrast Med. Mol. Imaging* **2006**, 1, 128–137.
- [21] I. Solomon, *Phys. Rev.* **1955**, 99, 559–565.
- [22] N. J. Bloembergen, *J. Chem. Phys.* **1957**, 27, 572–573.
- [23] J. H. Freed, *J. Chem. Phys.* **1978**, 68, 4034–4037.
- [24] L. Vander Elst, A. Sessoye, S. Laurent, R. N. Muller, *Helv. Chim. Acta* **2005**, 88, 574–587.
- [25] J. Rohovec, M. Kývala, P. Vojtišek, P. Hermann, I. Lukeš, *Eur. J. Inorg. Chem.* **2000**, 195–203.
- [26] A. Bianchi, L. Calabi, C. Giorgi, P. Losi, P. Mariani, P. Paoli, P. Rossi, B. Valtancoli, M. Virtuani, *J. Chem. Soc., Dalton Trans.* **2000**, 697–705.
- [27] P. Táborský, P. Lubal, J. Havel, J. Kotek, P. Hermann, I. Lukeš, *Collect. Czech. Chem. Commun.* **2005**, 70, 1909–1942.
- [28] P. Táborský, I. Svobodová, P. Lubal, Z. Hnatejko, S. Lis, P. Hermann, *Polyhedron* **2007**, 26, 4119–4130.
- [29] K. Popov, H. Rönkkömäki, L. H. Lajunen, *Pure Appl. Chem.* **2001**, 73, 1641–1677.
- [30] J. Huskens, D. A. Torres, Z. Kovacs, J. P. André, C. F. G. C. Geraldes, A. D. Sherry, *Inorg. Chem.* **1997**, 36, 1495–1497.
- [31] J. Moreau, E. Guillon, J.-C. Pierrard, J. Rimbault, M. Port, M. Aplincourt, *Chem. Eur. J.* **2004**, 10, 5218–5232.
- [32] P. Vojtišek, J. Kotek, V. Kubiček, J. Rudovský, P. Hermann, I. Lukeš, *5th International Conference on f-elements (ICFE)*, 24.8.–29.8.2003, Geneva, Switzerland.
- [33] J. Rudovský, P. Cígler, J. Kotek, P. Hermann, P. Vojtišek, I. Lukeš, J. A. Peters, L. Vander Elst, R. N. Muller, *Chem. Eur. J.* **2005**, 11, 2373–2384.
- [34] K. Kumar, M. F. Tweedle, M. F. Malley, J. Z. Gougoutas, *Inorg. Chem.* **1995**, 34, 6472–6480.
- [35] Y. Wang, W. D. Horrocks, *Inorg. Chim. Acta* **1997**, 263, 309–314.
- [36] G. Schwarzenbach, *Complexometric Titrations*, Interscience, New York **1957**.
- [37] R. N. Muller, D. Declercq, P. Vallet, F. Giberto, B. Daminet, H. W. Fischer, F. Maton, Y. Van Haverbeke, in *Proceedings of ESMRMB, 7th Annual Congress*, Strasbourg, **1990**.
- [38] P. Vallet, *Relaxivity of Nitroxide Stable Free Radicals. Evaluations by Field Cycling Method and Optimisation*, Ph.D. Thesis, University of Mons-Hainaut, Belgium, **1992**.



- [39] M. Kývala, I. Lukeš, *International Conference Chemometrics '95*, Pardubice, Czech Republic, **1995**, p. 63; the full version of "OPIUM" is available at <http://www.natur.cuni.cz/~kyvala/opium.html>.
- [40] M. Kývala, P. Lubal, I. Lukeš, *IX<sup>th</sup> Spanish-Italian and Mediterranean Congress on Thermodynamics of Metal Complexes (SIMEC 98)*, Girona, Spain, **1998**.
- [41] A. E. Martell, R. M. Smith, R. J. Motekaitis, *NIST Database of Critically Selected Stability Constants*, v. 7.
- [42] M. Maeder, Y.-M. Neuhold, G. Puxty, P. King, *Phys. Chem. Chem. Phys.* **2003**, 5, 2836–2841.

Received: February 13, 2009  
Published Online: June 23, 2009